

Numerical simulation of insulating particles trajectories in a multifunctional electrostatic separator

M. Maammar¹, W. Aksa¹, M. F. Boukhoulda¹, S. Touhami¹, L. Dascalescu², T. Zeghloul²

¹Electrostatics and High Voltage Research Unit IRECOM,
University Djillali Liabes Sidi Bel Abbès 22000, Algeria

²Electrostatics of Dispersed Media Research Unit, Institut P', UPR 3346 CNRS-
University of Poitiers-ENSMA, Angoulême 16021, France
phone: (213) 656-909-496
e-mail: aksa86wessim@gmail.com

Abstract—Electrostatic separation is a technique based on the forces that the electric field acting on small charged or polarized particles. Several electrostatic machines have been developed over past decades, operating with different principles and treating various mixture types. The multifunctional electrostatic separator is one of the most efficient installations for the treatment of micronized materials. This work aims to numerically simulate the dynamic behavior of micronized insulating particles in this type of separator. The numerical model of the electrostatic field calculated by COMSOL is used in a MATLAB program to simulate particle trajectories under the effect of electrical and mechanical forces. The numerical simulation implemented takes into account the impact of the particles with the rotating electrode. The intensity and direction of the forces exerted on the particles in the high intensity electric field area determine their behavior and thus the quality of the separation.

Keywords— electrostatic separation, numerical simulation, multi-function separator, electric field, particles trajectories.

I. INTRODUCTION

Global energy consumption is growing exponentially, 390 tons of oil equivalent every second. This can cause economic and environmental crises. Establishing new resources has become essential in order to conduct real eco-restructuring actions [1]. The electrostatic separation technique is a process able to prepare waste recycling, in environmentally respectful conditions, at reduced operating and maintenance costs [2].

In order to meet industrial needs, a great deal of research has been done to develop efficient electrostatic separation processes for different types of granular materials : free fall electrostatic separators [3-4], drum separators [5], electrode-electrostatic separator with plate and drum electrode [6], tribo-aero-electrostatic separators (TAES) with vertical electrodes [7], free fall (TAES) [8], (TAES) with rotating discs [9] and conveyor separators [10]. The multifunctional electrostatic separator with conveyor electrode (fig 1) implements three charging mechanisms, related to the electrical properties of the materials to be treated [11]: triboelectric charging, corona discharge and electrostatic induction.

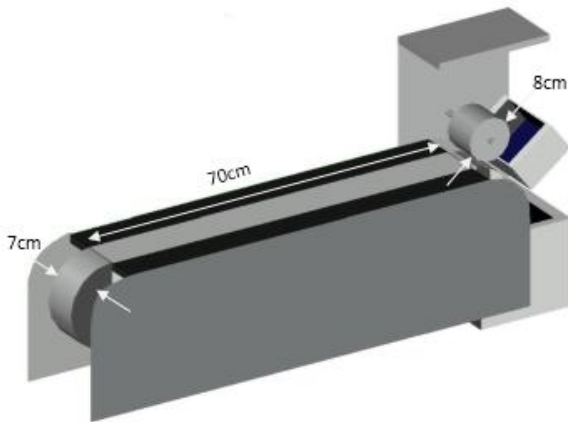


Fig. 1. Schematic representation of the multifunctional electrostatic separator with metal-belt conveyor

This installation is able to handle a large range of particle sizes, from powdery materials up to granular materials of millimeter sizes. Mixtures consisting of fine particles are deposited as a monolayer on the surface of a metal belt conveyor, which also plays the role of a grounded electrode. The conveyor is driven by a three-phase electric motor, controlled by a variable speed drive. The deposition of particles is achieved by an oscillating chute with dedicated control unit which has a particle dispersing device.

Various possibilities are available for this separator to charge particles. The choice of charging device will depend mainly on the electrical properties of the materials to be separated. The distinction between these materials will be made with respect to their conductivity which defines their ability to keep the charge acquired by triboelectric effect, by corona discharge or by electrostatic induction [11].

In this work we will develop a numerical simulation model of the particles trajectory in this multifunctional separator. The developed model uses the geometric and electrical data of the installation to define the position of the particles in the collector. This approach is useful for the design of the installation, and also to define its best performance, by optimizing the different stages of the process. The simulation is performed using the combination of the electric field calculation results from COMSOL with a MATLAB program as well as a number of simplifying assumptions that take into account the phenomena governing the behavior of particles in this type of separator.

II. SIMULATION MODEL

The installation used is represented by a stainless steel conveyor connected to the ground and a rotating cylindrical electrode connected to the high voltage. The position and inclination of the cylindrical electrode relative to the horizontal plane are adjustable.

To simulate the real behavior of particles in a multifunctional separator, we have developed a physical model of the particle trajectory in the electrostatic separation zone. In this installation, the particles are deposited on the surface of a metal belt conveyor. The movement of particles can be described by the equation (1) [7].

$$m \frac{d\vec{v}}{dt} = \sum \vec{F} \quad (1)$$

where m and v respectively represent the mass and velocity of the particle and $\sum F$ the sum of the forces acting on the particle. During their movements, the charged particles are subjected to an electrostatic force due to the action of the electric electric field prevailing in the interelectrode zone. The potential distribution in this area can be obtained by solving the Laplace equation (2) [12]:

$$\frac{\partial^2 V}{\partial x^2} + \frac{\partial^2 V}{\partial y^2} + \frac{\partial^2 V}{\partial z^2} = 0 \quad (2)$$

The intensity of the electrostatic field in the study area can then be derived from:

$$E = -\nabla V \quad (3)$$

In this study, the solution of (2) is obtained with specialized software for solving partial differential equations using the finite element method [13]. The results obtained by this method are shown in Figure 2.

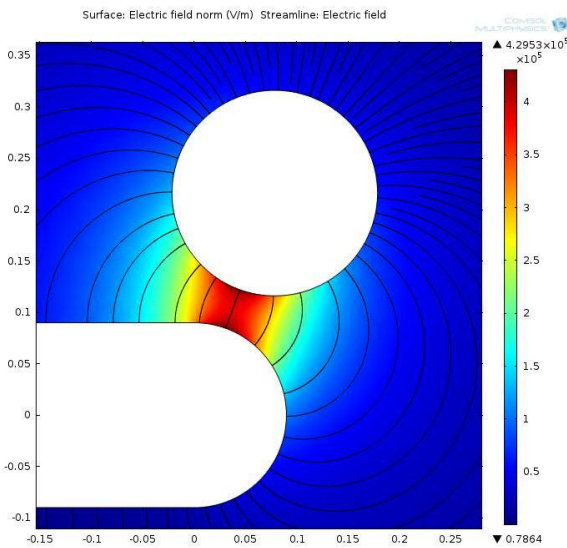


Fig. 2. Distribution and intensity of the electrostatic field

III. MOVEMENT OF PARTICLES IN A MULTIFUNCTION SEPARATOR

The movement of a charged particle in the electric field E applied to such an installation takes place under the action of several forces [14, 15]: gravitational force, electrostatic force, centrifugal force, electric image force and air-drag force.

A. Gravitational force

The gravitational force that acts on a particle of mass m is:

$$\vec{F}_g = \begin{bmatrix} 0 \\ mg \end{bmatrix} \quad (4)$$

where $g = 9.81 \text{ m/s}^2$ represents the acceleration of gravity.

B. Electrostatic force

The electrostatic force is evaluated by the experimental Coulomb law:

$$\vec{F}_{el} = Q\vec{E} = Q \begin{bmatrix} E_x(x, y) \\ E_y(x, y) \end{bmatrix} \quad (5)$$

Q is the electric charge acquired by the particles and $E(x, y)$ represents the electrostatic field in the separation zone [16].

C. Centrifugal force

This force tends to detach the particle from the conveyor surface. When the detachment of the particle occurs, this force vanishes.

$$\vec{F}_C = m_p \omega^2 R \vec{n} \quad (6)$$

m_p is the particle mass (kg), ω is the conveyor angular speed (rad/s) and R is the conveyor radius (m). The vector n represents the normal vector on the conveyor surface.

D. Electric image force

Under the action of this force, the charged particles are “pinned” to the conveyor. This force represents the Coulomb attraction between the charge Q the insulating particle acquired by ion bombardment and its image ($-Q$) situated at a distance $2r$ from it.

$$\vec{F}_m = \frac{Q^2}{4\pi\epsilon_0 2r^2} \vec{n} \quad (7)$$

ϵ_0 is the dielectric constant of the vacuum. ($\epsilon_0 = 8.854187 \times 10^{-12} \text{ F/m}$).

E. Air-drag force

The aerodynamic force applied to a homogeneous spherical particle can be evaluated by the following relation [17]:

$$\vec{F}_{ad} = \left(\frac{1}{2} C_f \cdot \rho \cdot S \cdot \vec{v}_r^2(x, y) \right) \vec{u} \quad (8)$$

where S represents the surface perpendicular to the air flow (m^2); v_r relative velocity of the particle (m/s); $\vec{u} = \vec{v}_r / v_r$ is the unit vector; $\rho = 1204 \text{ kg/m}^3$ is the density of the ambient air at 20°C ; C_f is the coefficient of friction

F. Shock velocities ratio

We have to determine the restitution coefficient [18], which depends on the materials nature and that appears during the separation of two solids A and B after collision. To account for this, we use a law due to Newton expressed by the ratio e of the relative velocities after and before the shock:

$$e = -\frac{v_A' - v_B'}{v_A - v_B} \quad (9)$$

where v_A, v_B represent the velocities before the shock; v_A', v_B' represent the velocities after the shock.

In our case, the two solids are: the particle and the wall of the rotating cylindrical electrode. Figure 3 gives a disposition of forces acting on two types of particles before and after take-off.

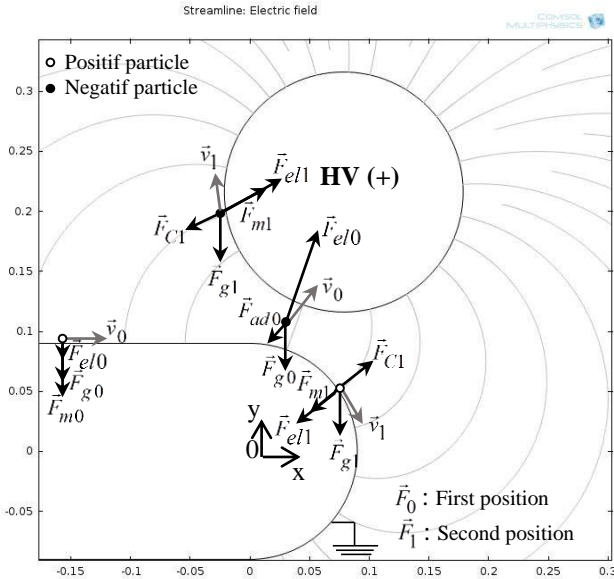


Fig. 3. Forces acting on a charged particle in the multifunctional separator

IV. NUMERICAL RESOLUTION OF MOVEMENT EQUATION

The approximate solution of the motion equation is obtained by substituting the equations (4-8) in (1):

$$\vec{a}(x, y) = \left(\frac{Q}{m}\right)\vec{E}(x, y) + (\omega^2 R)\vec{n} + \left(\frac{Q^2}{4m\pi\epsilon_0 2r^2}\right)\vec{n} - \left(\frac{C^{ST}\vec{v}_r^2(x, y)}{m}\right)\vec{u} \quad (10)$$

The system of equations (10) is solved using the finite difference method known as the Euler-Cromer algorithm [19,20]. The iterative scheme of the algorithm is described by equation (11):

$$\begin{aligned} v_{n+1} &= v_n + a_n \cdot \Delta t \\ p_{n+1} &= p_n + v_{n+1} \cdot \Delta t \end{aligned} \quad (11)$$

where a_n, v_n and p_n respectively represent the acceleration, the velocity and the position of the particles at time $n \cdot \Delta t$.

At the beginning of each iteration the initial value of the acceleration is calculated by equation (10) using the values of the exported electric field and the charge which is a parameter previously defined by an experimental measurement. This value is substituted in equation (11) for evaluating the position and velocity at instant Δt .

By using an interpolation algorithm, the electric field value is evaluated at the point p_n from the model based on the finite element method. So the acceleration at time Δt is calculated from the value of the electric field at point p_1 . Similarly, the velocity and position at time $2\Delta t$ can be evaluated from equation (11).

The simulation program is written under MATLAB and has several steps: 1) calculation of the electrostatic field using the finite element method (COMSOL software); 2) trajectory calculation by the Euler-Cromer method; 3) calculation of the coordinates at the point of impact of the particles with the wall of the rotating cylindrical electrode; 4) calculation of the position and velocity of the particle after the impact; 5) graphical representation of the results obtained. During the simulation, the particles are introduced into the electrostatic separation zone with an initial speed which corresponds to the conveyor speed; the value and direction of the velocity vector are considered as variable parameters. Table 1 shows the constant data taken during the simulation.

TABLE 1: SIMULATION PARAMETERS

Parameters	Values
Gravity acceleration	$g = 9.81 \text{ m/s}^2$
Voltage applied to the electrode	$V = 16 \text{ kV}$
Initial velocity of the particle	$v_p = 1 \text{ m/min}$
Friction coefficient	$C_f = 0.004$
Conveyor-electrode distance	$d = 0.015 \text{ m}$
Density of ambient air	$\rho = 1204 \text{ kg/m}^3$
Electrode Angle to the vertical	$\alpha = 20^\circ$

V. RESULTS AND DISCUSSION

Figure 4 shows the trajectories obtained by the simulation for different values of the charge Q . Increasing the charge enhances the attraction of the particle by the rotating electrode. A charge -5 pC is not enough for recovery at the cylinder, while a particle having a charge of -12 pC remains attached to the cylinder and is evacuated in the top collector. A positively charged particle $+10 \text{ pC}$ is subjected to a repulsive force by the rotating cylinder and remains “pinned” to the surface of the grounded conveyor belt.

We chose the clockwise direction as a positive direction, the rotation of the cylinder in this sense is convenient for recovering separated particles. The three simulations for the electrode speeds considered have the same detachment point and the same impact point with the rotating electrode. Excessive speeds such as 20 rpm and 40 rpm eject the particle out of their recovery zone (Figure 5).

The variation of the particle radius is shown in Figure 6. The decrease in the radius causes an increase in the electric image force, thus the particle of radius 0.1 mm sticks to the surface of the electrode while particles of 0.25 mm and 0.5 mm detach from the rotating electrode. A particle with a radius of 0.5 mm having a surface more exposed to the air-drag force than a particle of 0.25 mm , the latter pursues a trajectory in free fall.

The mass of the particle greatly influences its path as shown in Figure 7.

TABLE 2: COORDINATES OF DETACHMENT POINTS AS FUNCTION OF THE CHARGE

Electrode speed $n_{el} = 10$ rpm		
Particle radius $r = 0.3$ mm		
Particle mass $m = 0.5$ mg		
Detachment	$x[m]$	$y[m]$
$\triangleleft -12$ pC	-0.095	0.0903
$\triangleleft -6$ pC	0.002518	0.09026
$\triangleleft -5$ pC	0.01222	0.08947
$\triangleleft +10$ pC	0	-0.0903

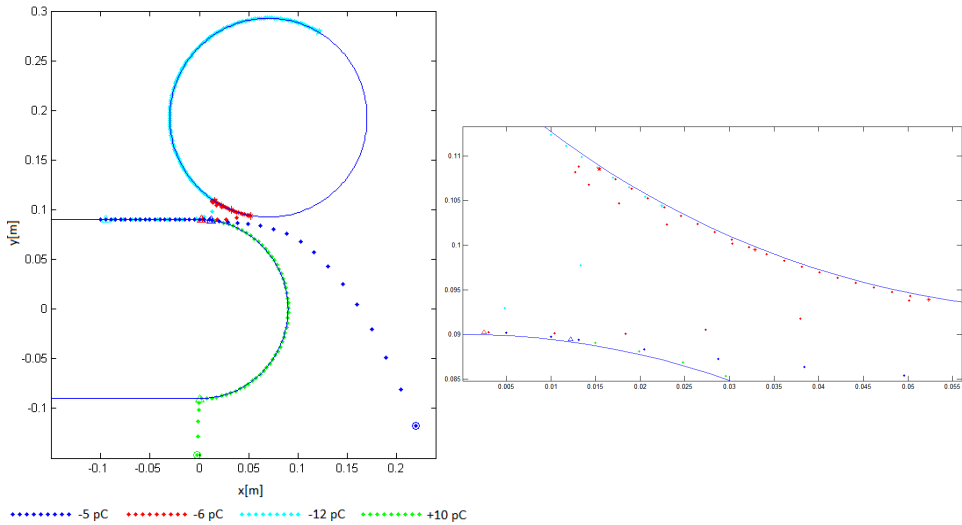


Fig. 4. Particle trajectories for various values of the charge Q (pC)

TABLE 3: COORDINATES OF DETACHMENT POINTS AS FUNCTION OF THE ROLL SPEED

Particle charge $Q = -0.6$ pC		
Particle radius $r = 0.3$ mm		
Particle mass $m = 0.5$ mg		
Detachment	$x[m]$	$y[m]$
$\triangleleft 10$ rpm	0.002518	0.09026
$\triangleleft 20$ rpm	0.002518	0.09026
$\triangleleft 40$ rpm	0.002518	0.09026

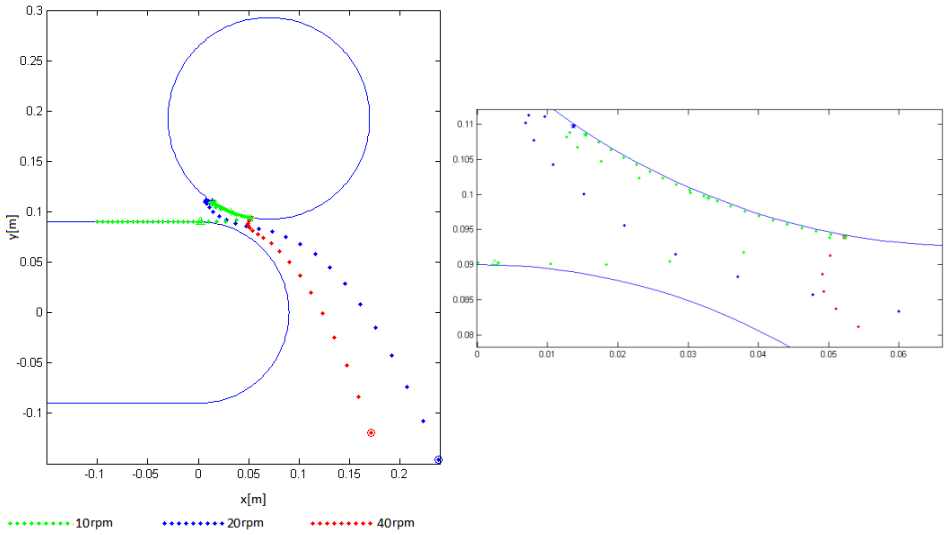


Fig. 5. Particle trajectories for various values of the rotating electrode speed (rpm)

Figure 8 shows the trajectory of ABS and PS particles having the same masses and sizes ($500\ \mu\text{m}$); the simulation data are derived from the results of the experimental studies: charge to mass ratio: $-15\ \text{nC/g}$ for PS and $30\ \text{nC/g}$ for ABS, high voltage applied to the rotating cylindrical electrode $V = 16\ \text{kV}$, distance between this electrode and the conveyor $d = 15\ \text{mm}$, rotational speed of the cylindrical electrode $n = 10\ \text{rpm}$ and speed of the metal conveyor $v = 1\ \text{m/min}$. ABS and PS particles that have opposite sign charges take distinct trajectories, their separation is successful.

TABLE 4: COORDINATES OF THE DETACHMENT POINTS AS FUNCTION OF THE PARTICLE RADIUS

Electrode speed $n_{el} = 10\ \text{rpm}$		
Particle charge $Q = -0.6\ \text{pC}$		
Particle mass $m = 0.5\ \text{mg}$		
detachment	$x[\text{m}]$	$y[\text{m}]$
\triangle 0.1 mm	-0.09499	0.0901
\triangle 0.25 mm	-0.000778	0.09025
\triangle 0.5mm	0.007161	0.09022

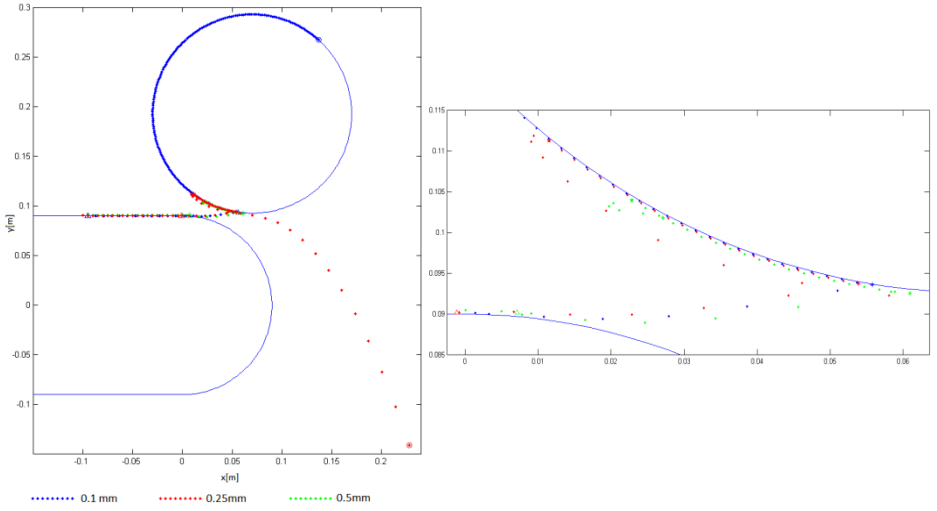


Fig. 6. Particle trajectories as function of the particle radius (mm)

TABLE 5: COORDINATES OF THE DETACHMENT POINTS AS FUNCTION OF THE PARTICLE MASS

Electrode speed $n_{el} = 10$ rpm		
Particle charge $Q = -0.6$ pC		
Particle radius $r = 0.25$ mm		
detachment	$x[m]$	$y[m]$
\triangle 0.1 mg	-0.09502	0.09025
\triangle 0.2 mg	-0.095	0.09025
\triangle 0.7 mg	0.01265	0.08936

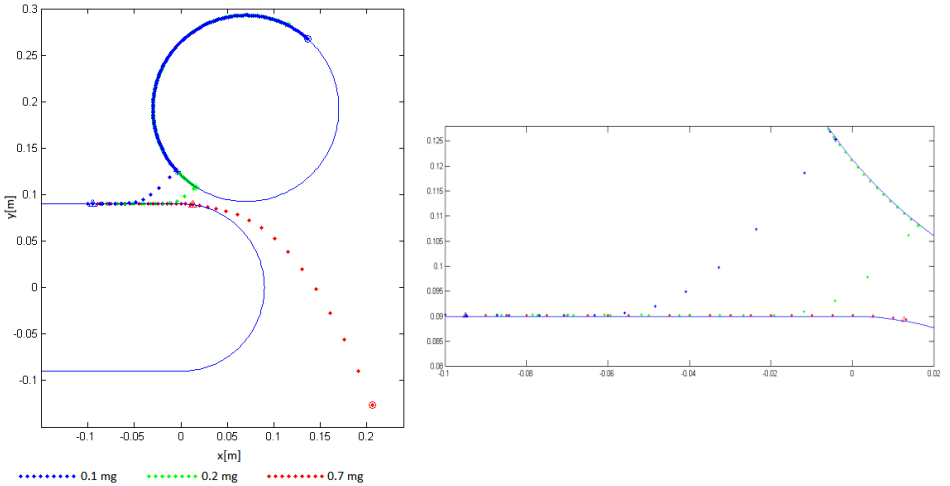


Fig. 7. Particle trajectories as function of the particle mass (mg)

TABLE 6: COORDINATES OF THE DETACHMENT POINTS OF THE ABS AND PS PARTICLES

Electrode speed $n_{el} = 10$ rpm Particle mass $m = 0.5$ mg Particle radius $r_p = 0.25$ mm		
detachment	x [m]	y [m]
\triangle ABS	-0.09484	0.09025
\triangle PS	0.07321	-0.05278

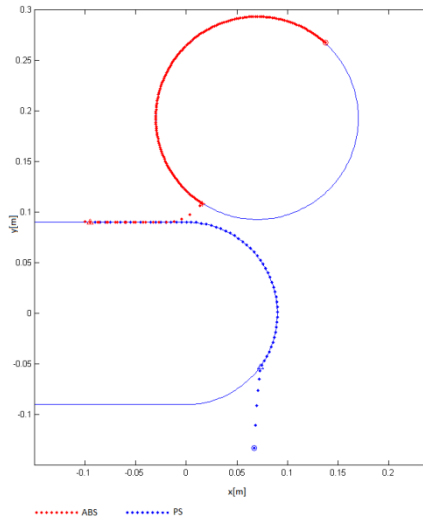


Fig. 8. Trajectories of ABS and PS particles

VI. CONCLUSIONS

The use of a MATLAB program that employs the electrical field data calculated by COMSOL Multiphysics has been proved to be effective for the numerical simulation of particle trajectories in a multifunctional separator. We were able to calculate the coordinates of the particle detachment points, their trajectories, and the possible impacts with the rotating electrode.

Numerical simulation of particle trajectories enabled the evaluation of the effects of several factors that affect the efficiency of the multifunctional electrostatic separator, in particular the charge acquired by the particles, the rotational speed of the rotating cylindrical electrode, the radius and mass of the particle. The results of the simulations are in good agreement with the results obtained experimentally on the same installation for a mixture of ABS and PS particles.

REFERENCES

- [1] S. Erkman, "Industrial ecology, a development strategy," *Sustainable Regional Research and Development*, Ed. University Presses François-Rabelais, FR: Tours, 2002, pp. 125-135.
- [2] R. Taurino, P. Pozzi, and T. Zanasi, "Facile characterization of polymer fractions from waste electrical and electronic equipment (WEEE) for mechanical recycling," *Waste Management.*, vol. 30, pp. 2601-2607, Dec. 2010.
- [3] Y. Higashiyama and K. Asano, "Recent progresses in electrostatic separation technology," *Part. Sci. & Technol.*, vol. 16, pp. 77-90, 1998.
- [4] A. Tilmatine, K. Medles, M. Younes, A. Bendaoud, and L. Dascalescu, "Roll-type versus free-fall electrostatic separation of tribocharged plastic particles," *IEEE Trans. Ind. Appl.*, vol. 46, pp. 1564-1569, 2010.
- [5] R. Kohnlechner, and L. Dascalescu, "new applications for standard electrostatic separators," in *Conf. Rec. IEEE Industry Applications Society 40th Annual Meeting, 2-6 Oct. 2005, Hong Kong*, vol. 4, pp. 2569-2572, 2005.
- [6] T. Zeghloul, S. Touhami, G. Richard, M. Miloudi, O. Dahou, and L. Dascalescu, "Optimal operation of a plate-type corona-electrostatic separator for the recovery of metals and plastics from granular wastes," *IEEE Trans. Ind. Appl.*, vol. 52, pp. 2506 - 2512, 2016.
- [7] S. Touhami, W. Aksa, K. Medles, A. Tilmatine, and L. Dascalescu, "Numerical Simulation of the trajectories of insulating particles in a tribo-aero-electrostatic separator," *IEEE Trans. Ind. Appl.*, vol. 51, no 2, pp. 4151- 4158, Sep./Oct. 2015.
- [8] Y. Hemery, X. Rouau, V. Lullien-Pellerin, C. Barron, and J. Abecassis, "Dry processes to develop wheat fractions and products with enhanced nutritional quality," *Journal of Cereal Science.*, vol.46, pp. 327-347, 2007.
- [9] A. Tilmatine, A. Benabboun, Y. Brahmi, A. Bendaoud, M. Miloudi, and L. Dascalescu, "Experimental investigation of a new triboelectrostatic separation process for mixed fine granular plastics," *IEEE Trans. Ind. Appl.*, vol. 50, pp. 4245-4250, 2014.
- [10] S. Messal, T. Zeghloul, A. Mekhalef Benhafssa, and L. Dascalescu, "Sorting of finely-grinded granular mixtures using a belt-type corona-electrostatic separator," *IEEE Trans. Ind. Appl.*, vol. 53, pp. 1424-1430, 2017.
- [11] S. Messal, R. Corondan, I. Chetan, R. Ouiddir, K. Medles and L. Dascalescu, "Electrostatic separator for micronized mixtures of metals and plastics originating from waste electric and electronic equipment," *Journal of Physics - Conference Series*, vol. 646, 2015.
- [12] W. Aksa, S. Touhami, M. Rezoug, K. Medles, L. Dascalescu, "Simulation numérique de la trajectoire des particules isolantes dans le séparateur tribo-aéro-électrostatique à deux étages" *10th Conference of the French Society of Electrostatic*, Poitiers, FR, Août 2016.
- [13] H. Labair, S. Touhami, A. Tilmatine, S. Hadjeri, K. Medles, L. Dascalescu, "Study of charged particle trajectories in free-fall electrostatic separators," *J. Electrostat.*, vol. 88, pp. 10-14, 2017.
- [14] M. Blajan, R. Beleca, A. Iuga, and L. Dascalescu, "Triboelectrification of granular plastic wastes in vibrated zigzag shaped square pipes in view of electrostatic separation," *IEEE Trans. Ind. Appl.*, vol. 46, no. 4, pp. 1558-1563, Aug. 2010.
- [15] S. Trigwell, M. K. Mazumder, and R. Pellissier, "Tribocharging in electrostatic beneficiation of coal: Effects of surface composition on work function as measured by X-ray photoelectron spectroscopy and ultraviolet photoelectron spectroscopy in air," *J. Vacuum Sci. Technol.*, vol. 19, no. 4, pp. 1454-1459, 2001.
- [16] Z. M. Xu, J. Li, H. Z. Lu, and J. Wu, "Dynamics of conductive and nonconductive particles under high-voltage electrostatic coupling fields," *Sci China Ser E-Tech Sci.*, vol. 52, no. 8, pp. 2359-2366, 2009.
- [17] C. Kevin, C. Muammer, T. M. Dario, C. Vincent, and O. Stephen, "Modelling of particle motion in an internal re-circulatory fluidized bed," *Chem. Eng. J.*, vol. 164, no. 2/3, pp. 393-402, Nov. 2010.
- [18] J. L. Fanchon, *Guide des Mécaniques. Sciences et Technologies Industrielles*. Paris, FR: Nathan, 1998, pp. 239.
- [19] H. Gould, J. Tobochnik, and W. Christian, *An Introduction to Computer Simulation Methods*. San Francisco, USA: Addison-Wesley, 2007.
- [20] J. Kiusalaas, *Numerical Methods in Engineering with MATLAB*. New York, USA: Cambridge Univ. Press, 2005.